



## Full Length Research Article

Advancements in Life Sciences – International Quarterly Journal of Biological Sciences

## ARTICLE INFO

## Open Access



Date Received:  
01/07/2023;  
Date Revised:  
07/09/2023;  
Date Published Online:  
20/10/2023;

# Investigation of the Impact of Environment Friendly Alumina Nanoparticles on Bacterial Activity

Taqwa Gh. Hamad, Taghried Ali Salman\*

**Authors' Affiliation:**  
Department of Chemistry,  
College of Science, Al-Nahrain  
University, Jadriya, Baghdad -  
Iraq

**\*Corresponding Author:**  
Taghried Ali Salman  
Email:  
dr.tag\_s@yahoo.com

**How to Cite:**  
Hamad TG, Salman TA  
(2023). Investigation of the  
Impact of Environment  
Friendly Alumina  
Nanoparticles on Bacterial  
Activity. Adv. Life Sci.  
10S(1): 95-100.

**Keywords:**  
Aluminum oxide  
nanoparticles; Green  
synthesis; Pomegranate  
leaves; *Staphylococcus  
aureus* bacteria

**Editorial Note:**  
You are viewing the latest  
version of this article having  
minor corrections related to  
the use of English language.

## Abstract

**Background:** *Staphylococcus aureus*, which is known as the most significant nosocomial pathogen and frequently causes postoperative wound infections, is a serious health issue in hospitals. *Staphylococcus aureus* has become increasingly drug resistant, and most of its strains have been shown to be resistant to practically all antibiotics. Numerous medical applications of aluminum oxide have been investigated, and this research indicates that the growth of *Staphylococcus aureus* may be inhibited in the presence of aluminum oxide nanoparticles.

**Methods:** The study was conducted from March 2023 to the end of July 2023 at Al-Aziziya Hospital in Iraq. Using spectrophotometry on microtiter plates, biofilms were created in vitro. Single isolated organisms of *Staphylococcus aureus* were examined for antibiotic susceptibility patterns using a conventional disk diffusion method. Furthermore, Prepared aluminum oxide nanoparticles were characterized using various techniques.

**Results:** The results show that strongly inhibited growth of *Staphylococcus aureus* in the presence of aluminum oxide nanoparticles after 24 hours at 0.06125, 0.1225, 0.245, and 0.49 M. On the other hand, X-ray diffraction analysis revealed an average crystallite size of 35 nm for the aluminum oxide nanoparticles. The FT-IR spectrum displayed prominent peaks at 615 and 636, corresponding to the stretching vibrations of aluminum oxide. The EDX measurements confirmed the presence of aluminum (Al) and oxygen (O) peaks, indicating the purity of the sample.

**Conclusions:** The antimicrobial assay demonstrated that the aluminum oxide nanoparticles exhibited significant antibacterial activity against *Staphylococcus aureus*. At a concentration of 0.06125 M of  $Al_2O_3$ , *Staphylococcus aureus* displayed a maximum zone of inhibition measuring 39 mm.



## Introduction

The production and characterization of nanoparticles have attracted significant scientific interest due to their unique features and potential applications, which differ from their bulk counterparts [1-5]. In the field of nano-biotechnology, there is currently active research focused on plant-mediated green chemistry [6, 7]. When regulated nanoparticles are taken up by plants, they can produce more stable nanoparticles with higher yields. Plant biosynthesis of nanoparticles requires careful consideration of factors such as temperature, pH, reaction time, plant extract quantity, and concentration of metal ions [8]. The market for nanoparticles (NPs) is projected to grow by 2025, particularly in the field of biomedical research focusing on metal oxide NPs [9]. The number of publications and patents related to the use of metal oxide NPs as medicinal agents and antibacterial agents has increased significantly in recent years [10]. There has been considerable interest in utilizing NPs as biosensors, for oncological diagnosis and treatment, and for drug delivery purposes [11, 12]. Metal oxide nanoparticles, including zinc oxide, iron oxide, titanium dioxide, silver oxide, and copper oxide, have demonstrated antibacterial properties, addressing bacterial infections, including antibiotic-resistant strains [13, 14, 15, 16]. Aluminum oxide nanoparticles ( $\text{Al}_2\text{O}_3\text{NPs}$ ), being the second interesting contender, have attracted attention due to their low cytotoxicity resulting from the inert nature of aluminum oxide [22, 23]. However, further research is needed to definitively establish their antibacterial activities. Due to its special qualities, such as strong mechanical strength, a large surface area to volume ratio, high hardness, and outstanding chemical stability, nanosized aluminum oxide ( $\gamma$ - and  $\alpha$ - $\text{Al}_2\text{O}_3$ ) is widely employed in a variety of industries [24, 25].  $\text{AlOxNPs}$  find applications as catalysts, adsorbents, components in concrete mixtures, tribological additives in lubricating liquids, raw materials for ceramics, and in industries such as cosmetics, textiles, and microelectronics [26, 27, 28, 29, 30, 31].  $\text{AlOxNPs}$  also hold potential in biomedicine, particularly as antibacterial agents [32, 33]. However, the mechanisms by which these nanoparticles affect microbial growth and development are not yet fully understood.

Typically, the biogenesis of nanoparticles happens when a plant's water-soluble extract goes through the bio reduction process with a water-soluble solution of the right metal salt. Fresh pomegranate leaf material was pro About 20–30 g of leaves was crushed with a mortar and pestle, and the resultant extract was filtered through muslin cloth. The extract was then maintained at room temperature for additional analysis [32]. cured from an Iraqi farm and cleaned thoroughly by being washed twice in distilled water. With a mortar

and pestle, about 20–30 g of leaves was crushed, and the resulting extract was filtered through muslin cloth. After that, the extract was kept at room temperature for further research [32]. The leaf extract contains flavonoids and phenolic acids with a variety of functional groups, which can act as reducing and stabilizing agents to produce nanoparticles.

Aluminum chloride was the primary chemical used to make aluminum oxide nanoparticles. The obtained extract was mixed with a saturated solution of aluminum chloride and allowed to sit for two hours in a magnetic stirrer (REMI, Laboratory Instruments) to ensure that the solutions were properly mixed. After stirring, the pH was measured to determine whether the extract's phytochemicals were reacting with the metal ions to form metal oxide nanoparticles. To settle the unused extract, the reaction mixture was next centrifuged at 2500 rpm for 20 minutes using a cooling centrifuge (REMI C-24 Plus). The resulting supernatant was then once more ultra-centrifuged at 14,000 rpm for 30 minutes.  $\text{Al}_2\text{O}_3\text{NPs}$  were produced by discarding the resultant supernatant and repeatedly washing the pellets in water and ethanol before drying them at 60 °C in a hot air oven as shown in Figure 1.

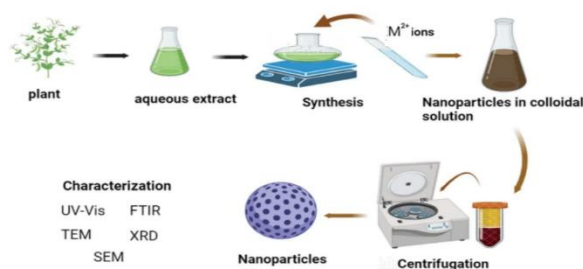


**Figure 1:** Green Synthesis of Metal oxide Nanoparticles.

In the present study, aluminum oxide nanoparticles ( $\text{Al}_2\text{O}_3$  NPs) loaded with green material were created using a straightforward biological reduction technique. The produced  $\text{Al}_2\text{O}_3$  NPs were characterized using a variety of widely used analytical and imaging techniques. Investigated was the nanoparticles' effectiveness as antibacterial against *Staphylococcus aureus*.

## Methods

### Plant extract preparation

A plant's aqueous extract is typically bio-reduced with an appropriate metal salt solution as part of the biogenesis of nanoparticles. Fresh pomegranate leaves for this investigation were procured from a farm and properly cleaned with distilled water to remove any impurities. The leaves were then around 20–30 grams in weight, and after being ground with a mortar and pestle, 100 ml of distilled water were added to the nano

powder. The extract was then kept at room temperature for upcoming tests. The extract of the leaves contains phenolic acids and flavonoids with a variety of functional groups that can act as both reducing and stabilizing agents, aiding the creation of nanoparticles.

### Synthesis of Alumina Nanoparticles

The primary chemical used in the synthesis of aluminum oxide nanoparticles was aluminum chloride from Merck, India. To ensure proper mixing of the solutions, the prepared plant extract was added to a saturated solution of aluminum chloride and stirred using a magnetic stirrer (REMI, Laboratory Instruments, India) for two hours. The pH of the mixture was monitored during the stirring phase to observe any changes, suggesting the occurrence of an interaction between the phytochemicals in the extract and the metal ions, leading to the creation of metal oxide nanoparticles. The resultant mixture was then treated to centrifugation at 2500 rpm for 20 minutes using a cooling centrifuge (REMI C-24 Plus) to separate the unused extract. The gained solution underwent additional processing by ultra-centrifugation for 30 minutes at 14,000 rpm. The pellets were then rinsed repeatedly with water and ethanol after the supernatant was removed. Aluminum oxide nanoparticles ( $\text{Al}_2\text{O}_3$  NPs) were then produced by drying the pellets in a hot air oven at 60 °C. A solution with a concentration of 0.490 M was then created by mixing a half gram of the produced nano powder with 10 ml of distilled water. Then, using three different doses of this solution, it was placed to plates for bacterial growth.

### Nanoparticles Characterization

A UV-1800 spectrophotometer from Shimadzo was used to measure the ultraviolet spectrum at room temperature. A Shimadzo FTIR 84005 spectrometer was used to obtain an infrared Fourier transform infrared (FTIR) spectrum. The plant extract containing aluminum oxide nanoparticles ( $\text{Al}_2\text{O}_3$ NPs) was dried at 60 °C for one hour before being combined with the proper quantity of KBr for FT-IR analysis. To verify the biogenesis of  $\text{Al}_2\text{O}_3$ NPs, X-ray diffraction (XRD) patterns were acquired using a Shimadzu XRD-6000 diffractometer. Using AA300 Angstrom AFM Atomic Force microscopy, the morphology and surface properties of the aluminum oxide nanoparticles were investigated. The SEM S-4160 electron microscope was also used to investigate aliquots of the plant extract filters containing aluminum oxide nanoparticles.

### Antibacterial Activity Studies

The antibacterial efficacy of aluminum oxide nanoparticles against *Staphylococcus aureus* was evaluated using the well-diffusion method. In

preparation for upcoming tests, the bacterial strain *S. aureus* was collected from the Korean Agriculture Culture Collection (KACC, South Korea). It was then kept on nutrient agar slants at 4 °C. The plate approach was used to inoculate the bacterial cultures. Brain heart infusion (BHI) broth was incubated at 37°C for 24 hours in the case of cultures. After that, Mueller-Hinton agar plates were used to cultivate the pathogenic bacteria. A sterile paper disk with a diameter of 5 mm was used to prepare each plate. Different concentrations of the manufactured aluminum oxide nanoparticles were added to the disks, with the plant extract serving as a control. The plates were then incubated for 24 hours at 37°C, and the inhibitory zones were measured and noted.

## Results

### Synthesized Aluminum Oxide Nanoparticles Characterization

FT-IR spectroscopy is a useful method for determining the amount of infrared light absorbed by a sample and displaying the results as a wavelength spectrum. Correlating the absorption bands (vibrational bands) with the chemical constituents present in the sample is necessary for the interpretation of the IR spectra [28]. The FTIR spectra for artificially created aluminum oxide nanoparticles is shown in Figure 2.

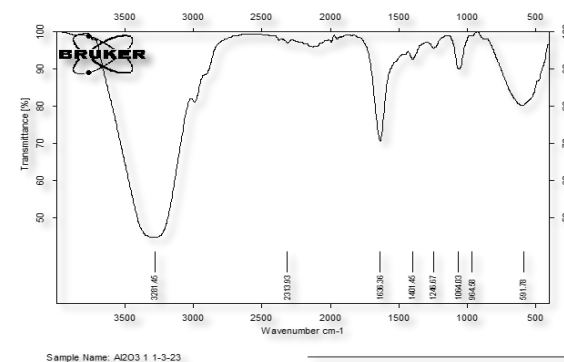


Figure 2: FT-IR spectra for aluminum oxide nanoparticles.

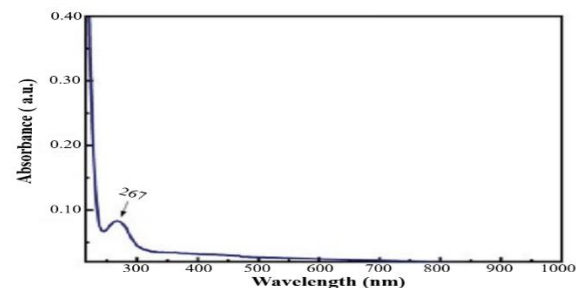
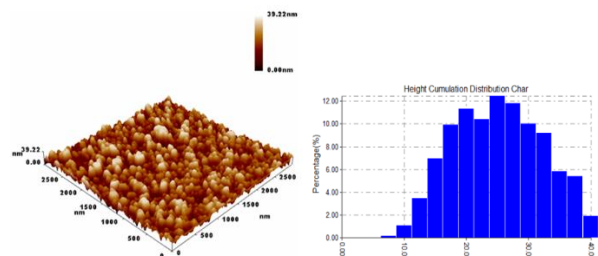


Figure 3: UV-visible spectra of  $\text{Al}_2\text{O}_3$  synthesis using Pomegranate leaves extract.

The UV-vis absorption spectrum of the produced nanoparticles was examined in order to estimate their optical energy band gap. A noticeable absorption peak (max) at 267 nm in the UV area was visible in the recorded spectrum, which supports the creation of aluminum oxide ( $\text{Al}_2\text{O}_3$ ) particles as shown in Figure 3.



**Figure 4:** AFM images of  $\text{Al}_2\text{O}_3$  synthesis using Pomegranate leaves extract.

AFM (Atomic Force Microscopy) analysis is employed to investigate the topography and surface characteristics of materials. It enables the generation of three-dimensional images that provide microscopic resolution of a nanoparticle's surface. In this study, AFM was utilized to examine the surface details of aluminum oxide nanoparticles ( $\text{Al}_2\text{O}_3$ NPs) synthesized using pomegranate leaf extract. Figure 4 presents a representative three-dimensional image illustrating the surface topography of the  $\text{Al}_2\text{O}_3$ NPs. The size, shape, and distribution of aluminum oxide nanoparticles synthesized using pomegranate leaf extract were examined using a scanning electron microscope (SEM). Figure 5 shows the results of the SEM investigation.

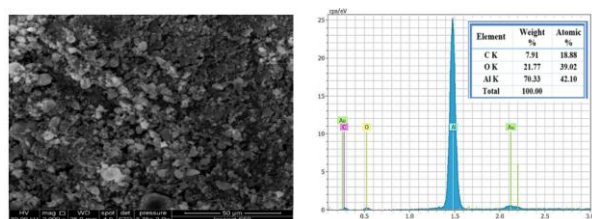


**Figure 5:** SEM and EDX images of  $\text{Al}_2\text{O}_3$  synthesis using Pomegranate leaves extract.

Figure 6 displays the aluminum oxide ( $\text{Al}_2\text{O}_3$ ) nanoparticles' diffraction peaks. The synthesized  $\text{Al}_2\text{O}_3$  NPs' XRD (X-ray diffraction) pattern exhibits a monoclinic structure and theta ( $\theta$ ) phase. The relative intensities of the observed diffraction peaks and the published values (JCPDS # 35-0121) are very similar to each other. The powder XRD pattern of  $\text{Al}_2\text{O}_3$  nanoparticles exhibits diffraction peaks at specific  $2\theta$  angles:  $18.96^\circ$ ,  $30.08^\circ$ ,  $38.57^\circ$ ,  $40.98^\circ$ ,  $44.74^\circ$ ,  $47.49^\circ$ ,  $54.94^\circ$ ,  $62.25^\circ$ ,  $63.25^\circ$ , and  $75.46^\circ$ , which correspond to the (102), (200), (104), (006), (015), (304), (311), (313), (306), (107), and (217) crystallographic planes, respectively. Applying the relationship  $D = 0.9/\cos$ , in which D is the crystalline terms of size, is the X-ray

irradiation wavelength, is the diffract angle, and is the complete width at half maximum height, the size of the  $\text{Al}_2\text{O}_3$  nanoparticles was calculated [26].

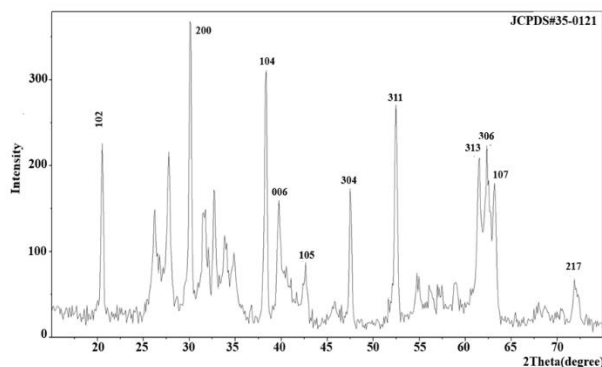


**Figure 6:** XRD Diffraction Pattern of  $\text{Al}_2\text{O}_3$  Nanoparticles.

To assess the antibacterial activity of aluminum oxide ( $\text{Al}_2\text{O}_3$ ) nanoparticles, *Staphylococcus aureus* (MCC 2408) was used as the target bacteria. The experimental results demonstrated that  $\text{Al}_2\text{O}_3$  nanoparticles synthesized through the sol-gel method exhibited significant antibacterial activity against bacteria. The results showed, as indicated in table 1, that the  $\text{Al}_2\text{O}_3$  nanoparticles' inhibitory effect grew stronger with decreasing concentration.

Conc./M	0.49000	0.24500	0.12250	0.06125
<i>Staphylococcus aureus</i>	No effect	Low kill	Kill	Kill

**Table 1:** Effect of different  $\text{Al}_2\text{O}_3$  nanoparticles concentrations against *Staphylococcus aureus*.

## Discussion

In this study, the stretching vibrations of aluminum oxide are thought to be responsible for the peaks seen at 615 and 636 as shown in figure 2. The sulfate ion's triply degenerate vibrational mode is associated with the peak at 1127. Furthermore, the water molecule's bending and stretching vibration modes are connected to the maxima at 1646 and 3526, respectively [30]. The reported absorption peak of  $\text{Al}_2\text{O}_3$  nanoparticles at 267 nm agrees with earlier research [7, 8].  $\text{Al}_2\text{O}_3$  nanoparticles were shown to have a significant absorption peak between 200 and 280 nm (258 nm) in which is consistent with description of a peak at 267 nm. Together, these results confirm that  $\text{Al}_2\text{O}_3$  nanoparticles were successfully formed in the current investigation, as shown by the significant absorption peak seen in the UV-vis spectrum at 267 nm. AFM image for synthesized nanoparticles reveals the nano-scale particle diameter, maintaining a 29.23 nm average size. The AFM analysis provides valuable insights into the morphology and structure of the synthesized  $\text{Al}_2\text{O}_3$  NPs, allowing for a better understanding of their physical properties and



potential applications. SEM results showed that the nanoparticles had a spherical form and range in size from 0.5 to 0.9 micrometers on average. This information provides valuable insights into the physical characteristics of the synthesized  $\text{Al}_2\text{O}_3$  nanoparticles and contributes to our understanding of their potential applications. Additionally, X-ray diffraction data discovered that the average crystallite size was 35 nm. Additionally, the calculated cell parameters of  $a = 0.5681$  nm,  $b = 0.2890$  nm, and  $c = 1.1776$  nm nearly match the values that were previously reported.  $\text{Al}_2\text{O}_3$  nanoparticles created by the bio reduction were measured using X-ray diffraction and their estimated size was found to be  $= (0.9180)/\cos \alpha$  (Figure 7). On the other hand, antibacterial behavior presented in table 1, revealed that the size of the inhibitory zone provides a clue as to how susceptible microorganisms are. These findings show how well  $\text{Al}_2\text{O}_3$  nanoparticles work to stop the spread of harmful germs and point to possible uses for them as antibacterial agents.

In this study, aluminum oxide ( $\text{Al}_2\text{O}_3$ ) nanoparticles with improved stability were created using a simple, low-cost green chemical process. This one-step technology is ideal for large-scale production since it does away with the complicated steps required by other organic techniques that use fungi and bacteria. By using XRD analysis, it was determined that the crystallite size of the described nanoparticles was 35 nm. The presence of aluminum oxide in the produced nanoparticles was confirmed by the FT-IR spectra and the EDX tests. It is interesting to note that the  $\text{Al}_2\text{O}_3$  nanoparticles showed mild antibacterial activity at low doses. According to these results,  $\text{Al}_2\text{O}_3$  nanoparticles could be used as a bacterial agent to control a variety of harmful organism's strategies.

## Acknowledgments

The authors would like to express their deepest gratitude to the Department of Chemistry, College of Science, Al-Nahrain University.

## Author Contributions

Taqwa Ghalib: writing-original draft, Data curation  
Taghried Salman: Supervision, methodology, Writing-Review and editing.

## Competing Interests

The authors declared that there were no conflictsof interest.

## References

1. Arakelyan S, Veiko V, Kutrovskaya S, Kucherik A, Osipov A, Vartanyan T, Itina T. Reliable and well-controlled synthesis of

- noble metal nanoparticles by continuous wave laser ablation in different liquids for deposition of thin films with variable optical properties. *Journal of Nanoparticle Research*, (2016);18:1-12.
2. Baalousha M, Fshinnia A, Guo L. Natural organic matter composition determines the molecular nature of silver nanomaterial-NOM corona. *Environmental Science: Nano*, (2018); 5(4): 868-881.
3. Neethu S, Midhun S, Radhakrishnan E, Jyothi's M. Green synthesized silver nanoparticles by marine endophytic fungus *Penicillium polonium* and its antibacterial efficacy against biofilm forming, multidrug-resistant *Acinetobacter* Bahmani. *Microbial pathogenesis*, (2018); 116: 263-272.
4. Devi L, Joshi S. Ultrastructure of silver nanoparticles biosynthesized using endophytic fungi. *Journal of Microscopy and Ultrastructure*, (2015); 3(1): 29-37.
5. Baghayeri M. Green synthesis of silver nanoparticles using water extract of *Salvia leriifolia*: Antibacterial studies and applications as catalysts in the electrochemical detection of nitrite. *Applied Organometallic Chemistry*, (2017).
6. Bindhu M, Umadevi M. Antibacterial and catalytic activities of green synthesized silver nanoparticles. *Spectrochemical Acta Part A: Molecular and Biomolecular Spectroscopy*, (2015);135: 373-378,
7. Edison T, Lee Y, Sethuraman M. Green synthesis of silver nanoparticles using *Terminalia cuneata* and its catalytic action in reduction of direct yellow-12 dye. *Spectrochimica Acta Part A: Molecular and Biomolecular Spectroscopy*, (2016);161: 122-129.
8. Ibrahim T, Taghried A, Salma A. Effectiveness of Magnesium oxide Nanoparticles in the Management of Thyroid Hormone Level. *Egyptian Journal of Chemistry*, (2021);64 (6): 2889 -2894.
9. Gudkov S, Burmistrov D, Smirnova V, Semenova A, Lisitsyn A. A Mini Review of Antibacterial Properties of  $\text{Al}_2\text{O}_3$  Nanoparticles. *Nanomaterials*, (2022);12(15): 2635-2641.
10. Singh S, Gill A, Nlooto M, Karpoomath R. Prostate cancer biomarkers detection using nanoparticles based electrochemical biosensors. *Biosensors and Bioelectronics*, (2019);137, 213-221.
11. Vimala D, Murugesan R, Francesco M, Antara B, Xiao F, Surajit P. Comparative study on anti-proliferative potentials of zinc oxide and aluminum oxide nanoparticles in colon cancer cells. *Acta BioMedica*, (2019); 90(2): 241.
12. Spirescu V, Chircov C, Grumezescu A, Vasile B, Andronescu E. Inorganic nanoparticles and composite films for antimicrobial therapies. *International Journal of Molecular Sciences*, (2021); 22(9): 459-464.
13. Xu, C. Applications of iron oxide-based magnetic nanoparticles in the diagnosis and treatment of bacterial infections. *Frontiers in Bioengineering and Biotechnology*, (2019); 7: 1-15.
14. Parks M, Messmer T. Characteristics of electronic cigarette users and their smoking cessation outcomes. *Cancer*, (2015);121: 800-810.
15. Raghunath A, Perumal E. Metal oxide nanoparticles as antimicrobial agents: a promise for the future. *International journal of antimicrobial agents*, (2017); 49(2): 137-152.
16. Marwah H, Taghried A. Kinetic and inhibition effect studies of ecofriendly synthesized silver nanoparticles on lactate dehydrogenase and ferritin activity of waxy crude oil. *Egyptian Journal of Chemistry*, (2022); 65(6): 627 - 635.
17. Bobkov Y, Walker W, Cattaneo A. Altered functional properties of the codling moth *Orco* mutagenized in the intracellular loop 3. *Scientific Reports*, (2021); 11(1):1-16.
18. Gudkov S, Burmistrov D, Serov D, Rebezov M, Semenova A, Lisitsyn A. Do iron oxide nanoparticles have significant antibacterial properties. *Antibiotics*, (2021);10(7): 884-889.
19. Akhtar S, Shahzad K, Mushtaq S, Ali I, Rafe M, Fazal-ul-Karim S. Antibacterial and antiviral potential of colloidal Titanium dioxide ( $\text{TiO}_2$ ) nanoparticles suitable for biological applications. *Materials Research Express*, (2019); 6(10): 105409.
20. Shah A, Haq S, Rehman W, Waseem M, Shoukat S, Rehman M. Photocatalytic and antibacterial activities of *Paeonia emodin* mediated silver oxide nanoparticles. *Materials Research Express*, (2019); 6(4): 04200.

21. Mohamed A. Eco-friendly Myogenic Synthesis of ZnO and CuO Nanoparticles for in vitro antibacterial, antibiofilm, and antifungal applications. *Biological Trace Element Research*, (2021); 199(7): 2788-2799.
22. Sara H, Taghrid A. The influence of green synthesized zinc oxide nanoparticles on testosterone hormone. *Biochemical and Cellular Archives*, (2022); 22(1): 921-928.
23. Sliwinska A, Kwiatkowski D, Czarny P, Milczarek J, Toma M, Korycinska A, Sziemraj J, Sliwinski T. Genotoxicity and cytotoxicity of ZnO and Al<sub>2</sub>O<sub>3</sub> nanoparticles. *oxicology Mechanisms and Methods*, (2015); 25: 176-183.
24. Jiao W, Yue M, Wang Y. Synthesis of morphology-controlled mesoporous transition alumina derived from the decomposition of alumina hydrates. *Microporous and Mesoporous Materials*, (2012); 147:167-177.
25. Manikandan V, Jayanthi P, Priyadharshan A, Vijayapratha E, Anbarasan P, Velmurugan P. Green synthesis of pH-responsive Al<sub>2</sub>O<sub>3</sub> nanoparticles: Application to rapid removal of nitrate ions with enhanced antibacterial activity. *Journal of Photochemistry and Photobiology A: Chemistry*, (2019); 371:205-215.
26. Nasrollahzadeh M, Issaabadi Z, Sajadi M. Green synthesis of Cu/Al<sub>2</sub>O<sub>3</sub> nanoparticles as efficient and recyclable catalyst for reduction of 2,4-dinitrophenylhydrazine, Methylene blue and Congo red. *Composites Part B: Engineering*, (2019); 166:112-119.
27. Ezati F, Sepehr E, Ahmadi F. The efficiency of nano-TiO<sub>2</sub> and γ-Al<sub>2</sub>O<sub>3</sub> in copper removal from aqueous solution by characterization and adsorption study. *Scientific Reports*, (2021); 11:18831.
28. Saliani M, Honarbakhsh A, Zhiani R, Movahedifar S, Motavalizadehkakhky, A. Effects of GO/Al<sub>2</sub>O<sub>3</sub> and Al<sub>2</sub>O<sub>3</sub> nanoparticles on concrete durability against high temperature, freeze-thaw cycles, and acidic environments. *Advances in Civil Engineering*, (2021); 1-12.
29. Kalneus V, Nemushchenko D, Larichkin V, Briutov A. Research of Physical and Mechanical Properties of Fly Ash Ceramics with SiO<sub>2</sub> and Al<sub>2</sub>O<sub>3</sub> Nanoparticles as Functional Addition. In *Key Engineering Materials*, (2021); 887: 528-535.
30. Sara H, Taghrid A. The potential of green-synthesized copper oxide nanoparticles from coffee aqueous extract to inhibit testosterone hormones. *Egyptian Journal of Chemistry*, (2022); 65(4): 395 - 402.
31. Ahmed S, Ahmad M, Swami B, Ikram S. Green synthesis of silver nanoparticles using *Azadirachta indica* aqueous leaf extract. *Journal of radiation research and applied sciences*, (2016); 9(1): 1-7.
32. Numan A, Ahmed M, Galil M, Al-Qubati M, Raweh A, Helmi E. Bio-Fabrication of silver nanoparticles using *Catha edulis* extract: procedure optimization and antimicrobial efficacy encountering antibiotic-resistant pathogens. *Advances in Nanoparticles*, (2020); 11(2): 31-54.
33. Bindhu M, Umadevi M, Esmail G, Al-Dhab N, Arasu M. Green synthesis and characterization of silver nanoparticles from *Moringa oleifera* flower and assessment of antimicrobial and sensing properties. *Journal of Photochemistry and Photobiology B: Biology*, (2020); 205: 111836.



This work is licensed under a Creative Commons Attribution-NonCommercial 4.0 International License. To read the copy of this license please visit: <https://creativecommons.org/licenses/by-nc/4.0/>